



## ORIGINAL RESEARCH

# Hybrid frequency control strategies based on hydro-power, wind, and energy storage systems: Application to 100% renewable scenarios

José Ignacio Sarasua<sup>1</sup> | Guillermo Martínez-Lucas<sup>1</sup>  | Hilel García-Pereira<sup>1</sup> |  
Gustavo Navarro-Soriano<sup>2</sup> | Ángel Molina-García<sup>3</sup>  | Ana Fernández-Guillamón<sup>3</sup>

<sup>1</sup> Department of Hydraulic, Energy and Environmental Engineering, Universidad Politécnica de Madrid, Madrid, Spain

<sup>2</sup> CIEMAT, Spanish National Research Centre on Energy, Environment and Technology, Madrid, Spain

<sup>3</sup> Department of Automatics, Electrical Engineering and Electronic Technology, Universidad Politécnica de Cartagena, Cartagena, Spain

**Correspondence**

Ángel Molina-García, Department of Automatics, Electrical Engineering and Electronic Technology, Universidad Politécnica de Cartagena, 30202 Cartagena, Spain.  
Email: [angel.molina@upct.es](mailto:angel.molina@upct.es)

**Funding information**

Comunidad de Madrid, Grant/Award Number: APOYO-JOVENES-SU3JLM-61-6XFZ49; Council of Communities of Castilla-La Mancha, Spain, Grant/Award Number: SBPLY/19/180501/000287; FEDER; SEPE (Spanish National Unemployment System)

**Abstract**

Over the last two decades, variable-speed wind turbines (VSWTs) have gradually replaced conventional generation. However, the variable and stochastic nature of wind speed may lead to large frequency deviations, especially in isolated power systems with high wind energy integration, where this integration causes a lack of inertia. This paper proposes a hybrid hydro-wind-flywheel frequency control strategy for isolated power systems with 100% renewable energy generation, considering both variable wind and a generator tripping. VSWTs and flywheels include a conventional inertial frequency control. The frequency control strategy involves VSWTs rotational speed and State of Charge (SOC) of flywheels variations that may affect the wear and tear of mechanical elements and reduce the efficiency of the frequency control action. The hydro-power controller also tracks the VSWTs' rotational speed deviation and the flywheel SOC to modify the generated power accordingly. This hybrid frequency strategy significantly reduces frequency excursions, the rotational speed deviations of VSWTs and the SOC of flywheels. To reduce the hydro-power plants' wear, an additional control strategy is proposed by the authors and evaluated. Results from a case study based on an isolated power system located in El Hierro (Canary Islands, Spain) are included, and extensively discussed in the paper.

## 1 | INTRODUCTION

Energy transition is the result of the depletion of fossil fuels, the need to reduce greenhouse gas emissions, and the aim of most countries of being energy-independent [1, 2]. Among the different renewable energy sources (RES), wind power plants—and, specially, variable speed wind turbines (VSWTs)—have become a common resource in the generation mix of most developed countries [3, 4]. However, VSWTs are connected through power converters which electrically decouple them from the grid and, subsequently, not directly contribute to the synchronous inertia of the power system [5]. As conventional power plants are replaced by VSWTs, the power system tends to stress in terms

of frequency stability and reliability due to the inertia reduction [6]. In fact, power systems with low synchronous inertia are related to a faster rate of change of frequency (RoCoF) and larger frequency deviations [7]. As a consequence, a variety of maximum instantaneous penetration limit for variable RES (vRES)—which include VSWTs and PV power plants [8]—can be found in the specific literature. For instance, Hewicker et al. estimated an averaged production mix across Europe with 50% RES in 2030 (of which 30% would come from vRES) [9]. The Australian National Electricity Market expects to be operated securely with up to 75% instantaneous penetration of vRES by 2025, if all recommended actions are fully taken [10]. Japanese Policy targets penetration of RES aims to reach 22–24% of

This is an open access article under the terms of the [Creative Commons Attribution-NonCommercial-NoDerivs](https://creativecommons.org/licenses/by-nc-nd/4.0/) License, which permits use and distribution in any medium, provided the original work is properly cited, the use is non-commercial and no modifications or adaptations are made.

© 2021 The Authors. *IET Renewable Power Generation* published by John Wiley & Sons Ltd on behalf of The Institution of Engineering and Technology

power production by 2030 [11]. Luo et al. affirm that the selection of each specific operation mode is mainly based on the forecasts of the power demand and renewable power generation, being the expected renewable energy penetration maximised in excess of 60% if sufficient renewable generation units and storage capacities are installed [12]. Nevertheless, most authors conclude that those conventional/synchronous power plants that currently provide frequency control to the grid (i.e. hydro-power, thermal, nuclear...), will suffer significantly from an increase of their wear as vRES increase their integration into power systems [13–18].

To mitigate power quality, reliability, and operation issues due to highly intermittent nature of vRES, a variety of energy storage systems (ESSs) have been widely proposed and used in power system [19]. Moreover, the use of kinetic energy directly provided by wind turbines has been also explored [20–22]. Among the different ESSs, flywheels have some remarkable benefits, such as fast response speed ( $\leq 10\text{ms}$ ), high energy efficiency (93–95%) and power density (1000–5000 W/L), low maintenance, environment-friendly features, and long lifetime [23]. In contrast to electro-chemical energy storage systems, flywheels are ideal to utility-scale storage systems due to their high power rating and quality, superior depth of discharge, and number of lifetime charge cycles [24]. Delille et al. admit that flywheels and batteries are also capable of providing similar dynamic performance to ultra-capacitors [25]. Disadvantages in comparison to ultra-capacitors are mainly focused on their instantaneous output is not very high, since devices with permanent magnet are commonly used in the rotor to remove the losses based on the magnetic coupling in the device [26, 27]. The most suitable applications of flywheels are focused on high power for a short duration and frequent charge–discharge cycles, such as hundreds of kW/10s of seconds [28]. Recent technology progress focused on reducing the self-discharge and performing ancillary services gives the flywheels the additional possibility to be considered for frequency and voltage regulation and support [29, 30]. Different contributions provide flywheel energy storage systems (FESSs) control strategies to enhance grid and transient stability [31–33], frequency regulation services [34–37], and automatic generation control in multi-area systems [38, 39]. Studies related to non-linear control of flywheels can be also found in [40].

According to the specific literature and to the best knowledge of the authors, there is a few of contributions focused on hybrid frequency control strategies considering the wear of the elements under high renewable scenarios. The majority of works point out aspects mostly related to the control and sizing of fast responsive energy storage technologies for frequency control services [41, 42]. Only a few contributions discuss wear and tear on plant components from the supply-side under high renewable integration [43], while recognising potentially increased wear and tear issues associated with vRES integration and, subsequently, dynamic frequency performance degradation [44]. Under this framework, the present paper proposes a hybrid hydro-wind-flywheel frequency control strategy for isolated power systems with 100% renewable energy generation scenarios considering hydro-power plant's and FESSs wear

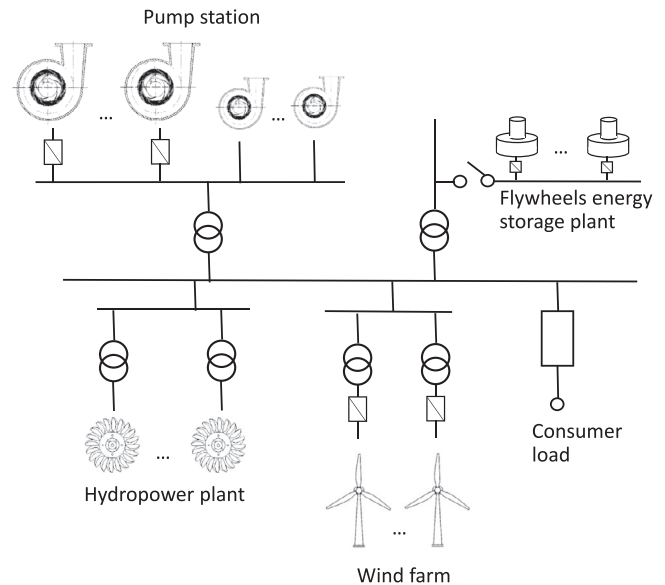


FIGURE 1 Power system scheme: one-line diagram

reductions by maintaining minor frequency deviations. Both variable wind and a generator tripping are considered as well.

The paper is structured as follows: Section 2 describes the power system modelling, Section 3 presents the proposed hybrid controller to reduce the hydro-power wear and minimise frequency excursions, Section 4 provides detailed information regarding different generation mix scenarios to evaluate the proposed hybrid frequency control strategy, Section 5 compares the proposed solution facing other frequency control strategies in terms of frequency excursion parameters and wear of the elements, finally, Section 6 gives the conclusions.

## 2 | DYNAMIC MODEL

To analyse the different hybrid control strategies in an isolated power system, an aggregated inertial model is used to emulate the grid frequency deviations, as proposed in [45]. This assumption was used by authors in the El Hierro power system [46] and by O'Sullivan et al. in the Irish power system modelling [47].

This isolated system, and consequently the model developed in Matlab Simulink [48], is composed of a hydro power plant, a pump station equipped with variable speed pumps (VSPs) and fixed speed pumps (FSPs), a wind power plant, a FESS, the Automatic Generation Control (AGC), the equivalent power system, and the power demand sensitive to frequency deviations, see Figure 1. The transmission lines' dynamics are neglected, since their influence on the grid frequency evolution is not significant [49]. The electromagnetic transients and electric machine dynamics are supposed to be much faster than the other components of the model; subsequently, their influence on the system's dynamics can be also ignored [50].

Frequency excursions are caused by imbalances between the power supplied by generator units and the power demand. Generation units are supposed to include hydroelectric units

( $p_b$ ) and wind turbines ( $p_w$ ). The generated power can be demanded by fixed speed pumps ( $p_{FSP}$ ), variable speed pumps ( $p_{VSP}$ ), as well as the consumers ( $p_D$ ), which include the under frequency load-shedding scheme. Consumer loads sensitivity to frequency variations are modelled through the  $D_{net}$  parameter. Frequency variations are formulated in Equation (1).

$$f \frac{df}{dt} = \frac{1}{2H_b} (p_b + p_w - p_{VSP} - p_{FSP} + p_f - p_D - D_{net} \Delta f), \quad (1)$$

where the  $2H_b$  term corresponds to the inertia constant of the hydroelectric units operating at each moment. Both VSPs and VSWTs, as well as the FESS, are connected to the grid through frequency converters, and thus, they are unable to naturally contribute to system frequency response [51]. Regarding FSPs, their associated electrical machines are asynchronous; consequently, their demanded power is clearly influenced by the electrical machine slip and the grid frequency. In order to take into account hydro-power plant and pump station hydraulic response, authors suggest models previously developed in [48, 52] and satisfactorily used in [46, 53]. Each VSWT is modelled considering the wind power model and both pitch and torque Maximum Power Point Tracking (MPPT) control, as presented in [54, 55]. For the rotor mechanical model, a one-mass rotor model is assumed, according to the recommendation proposed by Zhao and Nair [56] in cases in which the generator is decoupled from the grid through a power converter. A load shedding scheme is implemented in the model as, in an isolated power system with a high penetration of RES, frequency deviations may overpass thresholds associated with damage in both generation and demand equipment. This load-shedding scheme is based on the conventional Under Frequency Load Shedding (UFLS) scheme [57]. The RoCoF is also added as a complementary input.

A FESS model has been developed to be integrated with the rest of the system and perform a full analysis of the proposed hybrid frequency control. This model was previously used in [46, 58] in power system analysis. The FESS consists of  $n$  units of a flywheel energy storage system with the same electrical and mechanical characteristics. These flywheels work simultaneously and under the same operating conditions, starting from the same State Of Charge (SOC) and evolving in the same way. The losses of each unit are modelled based on the lab results of an industrial prototype. Mechanical losses of the flywheel, and the electrical losses of a switched electrical machine and its associated power electronics have been also considered for simulations [59]. The FESS model is parameterized with an initial SOC value. The input reference value is the required power, which is provided by the frequency regulation strategy described in Section 3. The output variables of the model are the instantaneous power supplied, the state of charge, and the available energy. The maximum electrical power capacity of the FESS depends on the state of charge, that is, the rated power can be managed at full charge condition (maximum speed) and the capacity decreases mostly linearly to half of the rated power value when the SOC is at 50%. In order to calculate this limit in the sup-

plied of stored electrical power, the efficiency of the flywheel is assumed as an efficiency map dependent on the SOC and the required power. In addition, a time delay in the power requirement is included in order to represent the dynamic response time of the control system and associated power electronics. The instantaneous evolution of the speed of the flywheel depends on inertia, the power supplied, and the self-discharge, which is a key parameter in this type of energy storage system. Finally, the available energy and the SOC are calculated from the speed value, which will be subsequently used as input by the proposed frequency control strategy to generate the FESS required power. It is then used by the FESS model as input.

### 3 | POWER-FREQUENCY CONTROL

Frequency control aims to minimise frequency variations due to power imbalances. With this aim, generation units within a power system must modify their power generation to provide the total demand and the system losses. The vast majority of European countries assume a frequency control system divided into two sequential actions: primary and secondary regulation. This frequency regulation can cause excessive stress on the electro-mechanical equipment of the generation units, as well as wear on the storage systems. For this reason, these classic controls are compared to the new proposed hybrid control loops, which also aim to minimise both wear and tear equipment.

In addition to the conventional frequency regulation provided by the generation units, frequency regulation can also be controlled from the demand-side since the power consumed by the pump station can be modified as needed. Therefore, frequency deviations are initially mitigated by hydroelectric units and VSPs according to the droop assigned to each unit. Permanent frequency error caused by the action of the primary frequency regulation is rectified by the secondary regulation, which is coordinated by the AGC. The AGC continuously sends increments of power reference to the hydroelectric units and VSPs. The control schemes of hydroelectric units, VSPs, VSWTs, and FESS are described in the following sections.

#### 3.1 | Conventional frequency control

The VSP controller consists of a PID controller modifying the power reference to be tracked by the power converter according to frequency and power deviations with respect to their references values, as indicated in Equation (2). This controller also includes the power reference obtained from the AGC, analogously to the hydroelectric units. On one hand, the permanent frequency error is corrected because of the action of both proportional and integral components of the PID controller, according to [46]. On the other hand, as VSPs are connected to the grid through a power converter, inertial behaviour must be emulated by the derivative component of the controller (synthetic inertia). In fact, VSP control action is

limited by the converter power limits.

$$\Delta p_{VSP} = \left[ K_{p,VSP} + K_{i,VSP} \int dt + K_{d,VSP} \frac{df}{dt} \right] (f - f_{ref}). \quad (2)$$

The steady grid frequency error resulting from the first control action (primary regulation) is managed by the AGC, which determines the second correction action (secondary regulation). In this power system, both hydro-power units and VSPs are aimed to provide this ancillary service. This control action is modelled in a similar way to [53].

### 3.2 | Inertial frequency control

VSWTs also provide synthetic inertia. Inertial frequency regulation adds an auxiliary signal, sensitive to frequency, to the reference power set-point in VSWTs, momentarily increasing wind turbine output power at the expense of slowing down the rotor speed. The joint inertial and proportional VSWT control strategy proposed in [60] is assumed. As VSWTs are connected to the system through a power converter, the PD control loop adds a power signal  $\Delta p_{w,f}$  to the power reference output to be tracked by the converter (Equation (3)):

$$\Delta p_{w,f} = \left[ K_{p,wf} + K_{d,wf} \frac{df}{dt} \right] (f_{ref} - f). \quad (3)$$

The variation of power injected by the VSWTs into the grid  $p_{w,f}$  causes variations of the rotational speed. In addition, the generator torque control lets the variation of the wind turbine rotor speed following an MPPT strategy, for extracting as much power as possible from the wind flux [61]. Therefore, the deviation from the reference value of the rotational speed,  $\omega_{ref}$  [62], produced by VSWT inertial frequency regulation and the changes in wind speed conditions are corrected as described in expression (4) according to [55], which corresponds with a PI controller whose power signal is also tracked by the power converter.

$$\Delta p_{w,\omega} = \omega \left[ K_{p,\omega\omega} + K_{i,\omega\omega} \int dt \right] (\omega - \omega_{ref}). \quad (4)$$

Therefore, the total variation of power injected by VSWTs,  $\Delta p_w$ , corresponds to the sum of the increment of the power due to the inertial control loop,  $\Delta p_{w,f}$ , and the increment of power due to the rotational speed control loop,  $\Delta p_{w,\omega}$ .

Figure 2 shows both PD and PI control loops of the VSWTs. According to [53], VSWTs contribution both to primary or secondary regulation implies a reduction in wind power generation due to reserve requirements. Nevertheless, these contributions are not considered in this paper. Regarding FESS frequency control, it consists of an inertial controller—see equation (5), analogous to the controller implemented in VSWTs as shown in Figure 3.

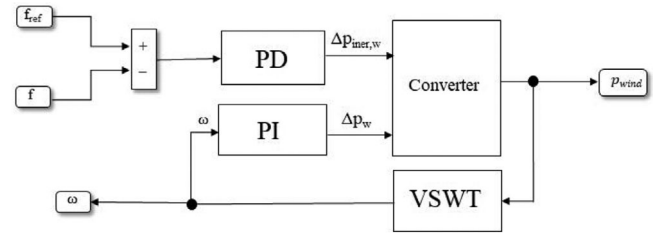


FIGURE 2 VSWT modelling: Controllers detail

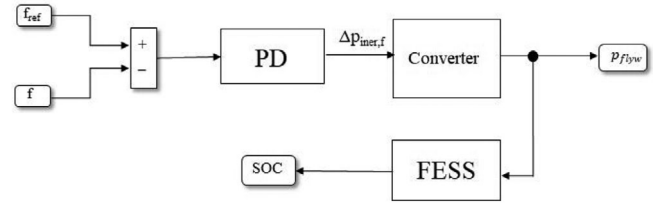


FIGURE 3 FESS modelling: Controller detail

$$\Delta p_{FESS} = \left[ K_{p,F} + K_{d,F} \frac{df}{dt} \right] (f_{ref} - f). \quad (5)$$

### 3.3 | Proposed hybrid controller

As previously mentioned in Section 3.2, both VSWTs and FESS include an inertial frequency control. These controllers improve the grid frequency excursions, but causes the rotational speed of VSWTs and the SOC of FESSs to deviate from their reference values. With regard to the VSWTs, the PI speed controller must minimise the rotational speed error, reducing the effectiveness of the frequency inertial control, together with an increase in the VSWTs' wear [63, 64]. On the other hand, FESS become unloaded over time. In order to mitigate these issues, a new frequency control strategy for hydro-power plants is proposed in this work. Apart from the PI-controller used for primary and secondary frequency regulations, two new control loops are added to the hydro-power conventional governor. In this way, VSWTs' rotational speed error and FESS' SOC are the two new inputs, which are corrected by the constant gains  $K_{p,\omega,hyd}$  and  $K_{p,soc,hyd}$ , respectively, and added to the PI conventional control, see Figure 4. Similar strategies were previously proposed in [65], where a cooperation between hydro-power plants and FESSs was analysed. In addition, the authors suggested an alternative frequency strategy for PV power plants in [66], where the frequency controller included the VSWTs' rotational speed deviation as an input; and a coordination between hydro-power and VSWTs in [67].

The proposed hybrid frequency control scheme reduces significantly the grid frequency excursions, simultaneously improving the PD inertial control effectiveness of both VSWTs and FESS. However, this hybrid approach implies an increase in the hydro-power generation units' wear, which is measured through the nozzle deviations [50]. Consequently, an additional dead-band is added to the proposed hydro-power controller, as



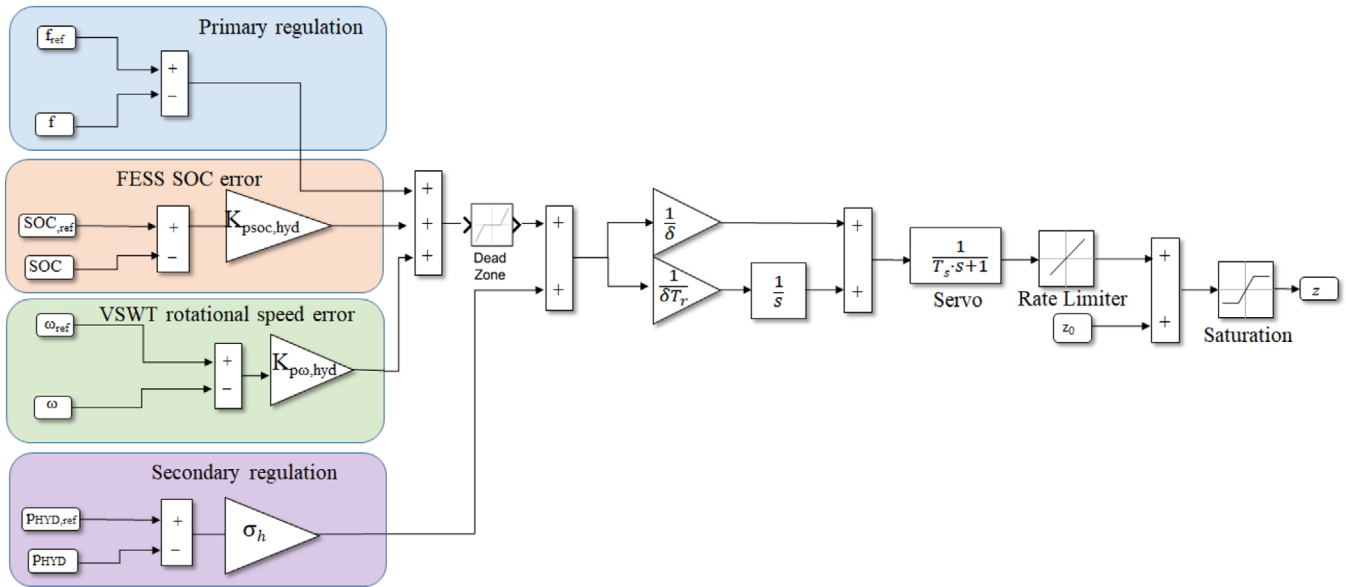


FIGURE 4 Proposed hybrid frequency controller

shown in Figure 4. This dead-band avoids hydro-power plant to participate in frequency regulation, if the input is within a specified range, and subsequently the hydro-power plant wear is reduced. In addition, the dead-band also influences in the input of the deviation of the frequency, the SOC of FESS and the VSWTs rotational speed. Some suitable values of the frequency limits of such dead-band are analysed and discussed in Section 5.3.

#### 4 | CASE STUDY: GENERATION MIX SCENARIOS

To evaluate the suitability and compare the proposed controller, different scenarios are simulated to cover all the operating modes of the power system under study. In this case, it is assumed that the supply-side of the isolated power system is 100% renewable.

Analogous to authors' previous contributions [46, 68], the proposed new hybrid control loop is evaluated considering the real isolated power system placed in El Hierro, Canary Islands (Spain). The island demand, which fluctuated between 7.7 MW and 2.1 MW in 2018, has been commonly covered by diesel groups (11.2 MW rated power). However, this island is a UNESCO (United Nations Educational, Scientific, and Cultural Organisation) biosphere reserve since 2000, and thus, RES integration has been then considered a priority target. In 2014, 'Gorona del Viento' wind pumped storage power plant was commissioned with five 2.3 MW ENERCON E-70 Type 4 VSWTs. The pumped storage power plant was equipped with  $4 \times 2.8$  MW Pelton turbines,  $6 \times 0.5$  MW FSPs, and  $2 \times 1.5$  MW VSPs; further information can be found in [46]. The renewable power supply-side has increased notably last years. In [69], collected data from El Hierro power system showed

that wind speed ramps may address the loss of 1.6 MW (from 3.0 MW to 1.4 MW) in 5 s. These events involve the activation of load shedding control actions, which is commonly used in El Hierro under such frequency circumstances, especially using FSPs. Nowadays, VSPs take also part in primary and secondary frequency regulation. In this context, the proposed hybrid frequency control scheme is assessed in this isolated power system as case study.

For the definition of representative scenarios for analysis purposes, a study of the power system demand is carried out, thus recorded data are used [53]. The selected realistic scenarios include various generation mixes that have taken place in El Hierro power system, such as hydraulic short circuit, among others [69]. It is well known that hydraulic short circuit is necessary to give stability to the grid frequency in cases in which wind penetration is very high, even though it is not an operation mode appropriate from the point of view of the water balance [70]. By considering that this work aims to analyse the power system under conditions of 100% renewable generation, generation mix scenarios in which there are diesel units under operation have been omitted. A total of 22 scenarios (100% renewable) proposed in [53] are then used in this work to analyse the suitability of the proposed hybrid controller.

To evaluate the benefits of this hybrid controller, two different contingencies are defined for each scenario, covering both the ordinary and extraordinary operation of the power system, respectively: (i) the fluctuation in the wind speed [68], and (ii) the sudden loss of the generating unit injecting the highest value of active power to the system, 'largest unit' [57]. Since the model includes the dynamic response of the VSWTs under wind speed fluctuations, the main input variable to the system is the wind speed ( $s_\omega$ ), and thus, a suitable simulation of wind evolution is crucial, particularly in the short-term. Due to the time frame considered in this work (600 seconds), a hybrid model for the

wind speed numerical generator proposed in [71] and satisfactorily used in [53] is assumed. This hybrid model is based on Van der Hoven's model [72] for the medium and long-term, and von Karman's turbulence model [73] for the short-term.

## 5 | RESULTS

The hybrid frequency control strategy proposed in Section 3.3 is evaluated and compared to other three strategies previously presented in the specific literature:

- **Base control:** grid frequency is only controlled by hydro-power plants and the VSPs, both including primary and secondary regulation. This is the current real power-frequency control of the case study under analysis (El Hierro, Spain).
- **Inertial control:** grid frequency is controlled by hydro-power plants and VSPs with primary and secondary controls, and by FESS and VSWTs with the inertial control.
- **Hybrid control:** grid frequency is controlled by hydro-power plants and VSPs with primary and secondary controls, and by FESS and VSWTs with the inertial control, including the hybrid control (rotational speed of VSWTs and SOC of FESS are sent to the hydro-power plant, see Figure 4).
- **Hybrid control with dead-band:** grid frequency is controlled by hydro-power plants and VSPs with primary and secondary controls, and by FESS and VSWTs with the inertial control, including the hybrid control (rotational speed of VSWTs and SOC of FESS are sent to the hydro-power plant, see Figure 4) and the dead-band.

First of all, the frequency excursions under wind speed variation and the loss of the largest power plant are studied under the four power-frequency control strategies. The time-frame under analysis is 10 min (600 s). The wear of the different elements is then determined. Finally, an analysis of the dead-band limits is carried out to determine which is the most suitable value to reduce the hydro-power plants' wear. At the same time, frequency deviations, rotational speed of VSWTs, and SOC of FESS are not very aggravated.

### 5.1 | Comparison of frequency control strategies

The four strategies are here analysed with the 22 generation mix scenarios presented in Section 4. A dead-band value of 100 mHz is selected for the **hybrid control with dead-band**. Section 5.3 analyses and justifies that the optimum values for the dead-band should range in between 50 and 100 mHz. According to the conclusions extracted from that section, the results would be slightly different depending on the selected dead-band value. However, this variability does not affect to the analysis developed in the present section, as the main characteristics regarding the parameters under consideration would be similar independently of the chosen dead-band value (as long as it is within that specified range). Two different situations are

considered: (i) variable wind speed; and (ii) constant wind speed and the loss of the largest power plant.

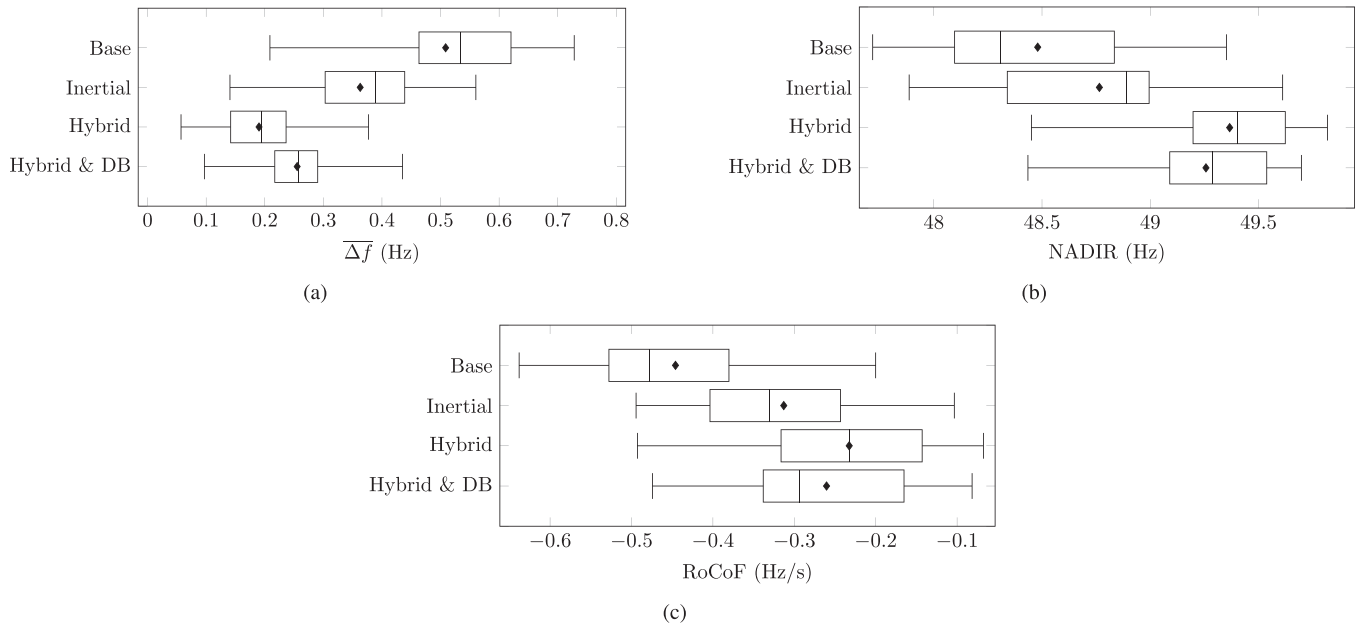
#### 5.1.1 | Variable wind speed

The power output change from VSWTs due to wind speed variation can cause continuous frequency fluctuations, especially in isolated power systems [74]. The parameters taken into account to compare the different frequency control strategies are:

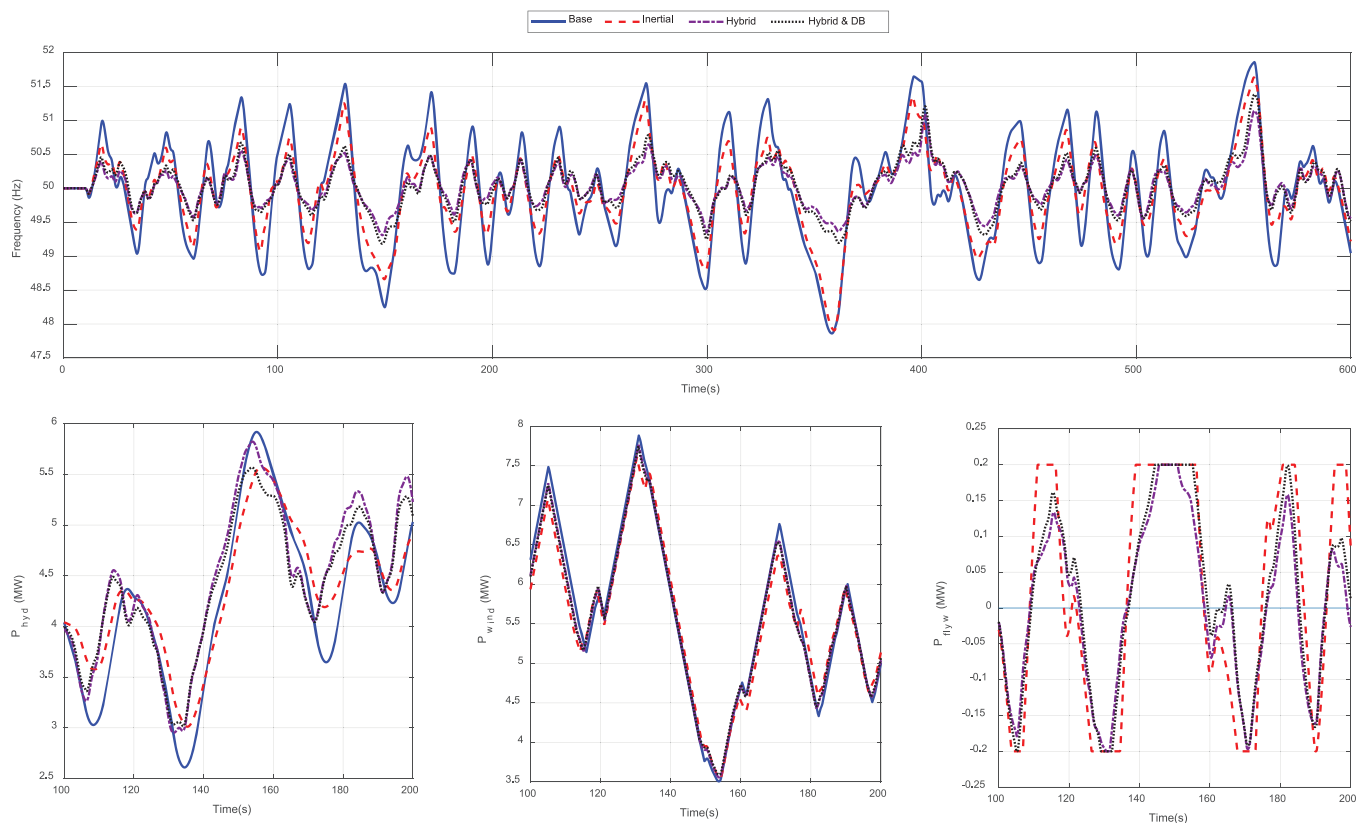
- Average frequency deviation ( $\overline{\Delta f}$ )
- Minimum frequency value (NADIR)
- Worst rate of change of frequency (RoCoF)
- Average hydro-power generation units' wear ( $\overline{\Delta z}$ )
- Number of cycles/h of FESS (cycles/h)
- Average state of charge deviation of FESSs ( $\overline{\Delta SOC}$ )
- Average rotational speed deviation of VSWTs ( $\overline{\Delta \omega}$ )

Figure 5 shows the frequency deviation parameters under analysis considering the 22 generation mix scenarios ( $\overline{\Delta f}$ , NADIR and RoCoF) as box-whisker plots. According to the results, the frequency deviation values improve as more elements are included in the control strategy, as was predictable. In fact, the **base control** provides the worst results in terms of  $\overline{\Delta f}$ , NADIR, and RoCoF. When flywheels and VSWTs are included with the **inertial control**, frequency response improves. However, the **hybrid control**, in which the hydro-power plant takes into account the  $\Delta \omega$  and  $\Delta SOC$ , gives the best results among the four strategies. The **hybrid control with dead-band** also provides a significant improvement to the **base control** and **inertial control**, but slightly worsens the results in contrast to the **hybrid control**. Indeed, NADIR and RoCoF are similar for both **hybrid control** and **hybrid control with dead-band**, but  $\overline{\Delta f}$  is increased. As an example of results for a specific generation mix scenario, Figure 6 depicts the graphical results of schedule number 20 in terms of frequency and active powers': hydro-power, wind, and flywheels. As can be seen, and in line with the results previously discussed, the maximum and minimum values of grid frequency are obtained for the **base control**, but they are improved when VSWTs and FESS contribute to frequency control. Both hybrid controls—**hybrid control** and **hybrid control with dead-band**—provide severe improvements and, actually, similar responses are obtained for them.

The other parameters can be seen in Figure 7. With regard to the  $\overline{\Delta z}$ , the best results are provided by the **inertial control**, and the worst by the **hybrid control**. These results are coherent with the different frequency control strategies: in the **inertial control**, hydro-power generation units only give primary and secondary frequency control, but as VSWTs and FESS are also participating with their inertial response, hydro-power regulation is reduced in comparison to the **base control**. On the contrary, with the **hybrid control**, an additional effort must be provided by hydro-



**FIGURE 5** Box-whisker plots for frequency deviations under variable wind speed. (a) Average frequency deviation. (b) NADIR. (c) RoCoF.



**FIGURE 6** Grid frequency and active power of hydro-power units, VSWTs, and FESSs

power units as they consider the  $\Delta\omega$  and  $\Delta SOC$ . The advantage of the dead-band's included in the hybrid control with dead-band is related to  $\overline{\Delta z}$ , reducing the nozzle deviations and giving similar values to those of the base control, as was

detailed and explained in Section 5.3. Considering the FESS, both number of cycles/h and  $\Delta SOC$  in the base control are null, as FESS do not contribute to frequency control in such strategy. Among the three other strategies, inertial

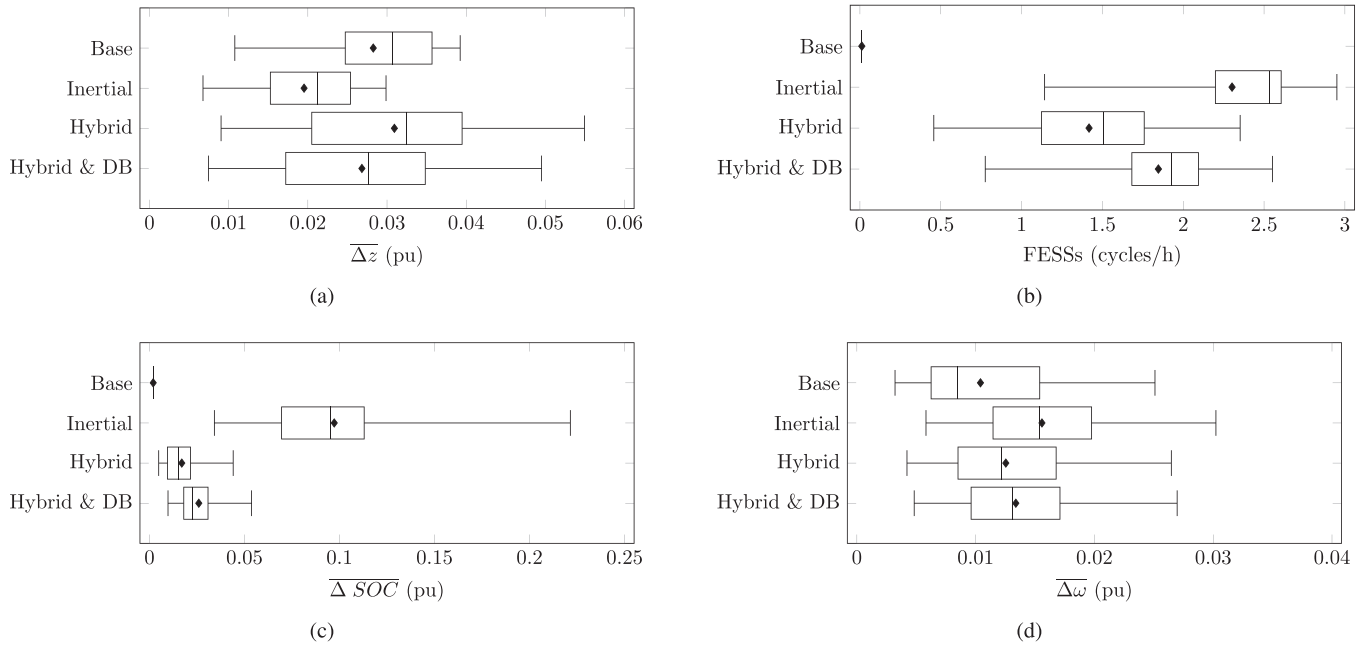


**FIGURE 7** Box-whisker plots for  $\overline{\Delta z}$ , number of cycles/h of FESSs,  $\overline{\Delta SOC}$ , and  $\overline{\Delta \omega}$ . (a) Average nozzle deviation. (b) FESSs cycles/h. (c) Average state of charge deviation of FESSs. (d) Average rotational speed deviation

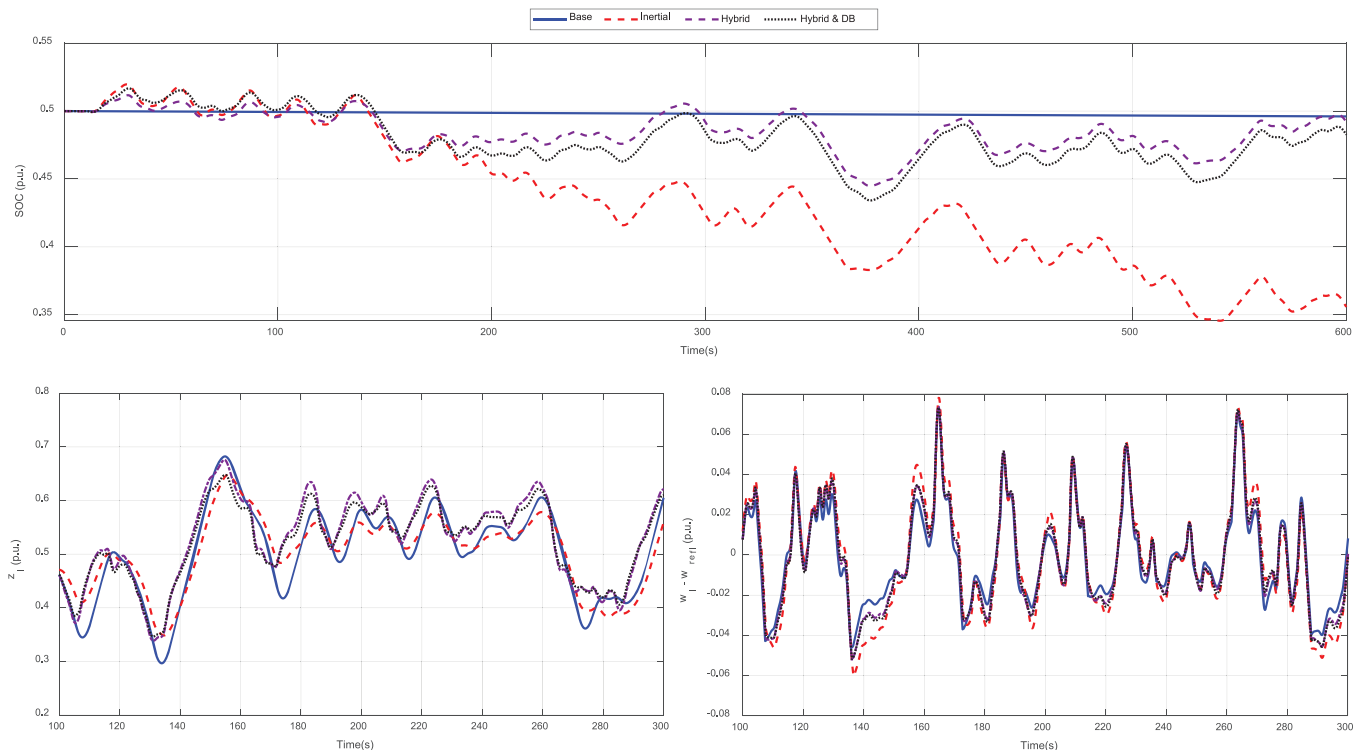


**FIGURE 8** State of charge of FESSs, nozzle position of hydro-power plants, and rotational speed deviation of VSWTs

control causes the FESSs to have the highest number of cycles/h and maximum  $\overline{\Delta SOC}$ . However, these values are in line with those data provided by the manufacturers [75]. The  $\Delta SOC$  is due to the progressive discharge of the FESS

when they provide the inertial control, as depicted in Figure 8. In contrast, both the hybrid control and the hybrid control with dead-band provide similar results, and the SOC does not deviate so much as in the inertial control.



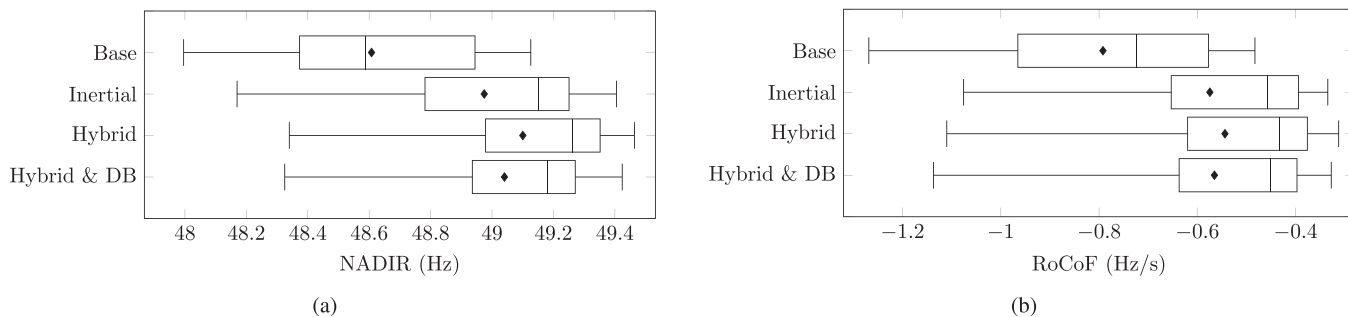


**FIGURE 9** Box-whisker plots for frequency deviations after the loss of the largest power generator. (a) NADIR. (b) RoCoF.

Finally, the rotational speed deviation of VSWTs in the **base control** is just due to the wind speed evolution. In line with the FESS, the **inertial control** causes the  $\overline{\Delta\omega}$  to have the maximum variations, whereas the **hybrid control** and the **hybrid control with dead-band** reduce such deviations to similar values to the **base control**. Figure 8 depicts the graphical results for these parameters for the schedule number 20, in a similar way to Figure 6. As can be seen, results previously detailed and explained are verified within the simulation.

### 5.1.2 | Loss of the largest power generator

The loss of the largest power generation unit is the most severe contingency in terms of frequency deviation, and it can cause load-shedding and even black-outs [76]. In this case, the parameters taken into account to compare the different frequency control strategies are:

- Minimum frequency value (NADIR)
- Worst rate of change of frequency (RoCoF)
- Number of schedules in which load shedding is activated (LS schedules)
- Number of load-shedding steps (LS steps)
- Power shed due to load-shedding ( $P_{shed}$ )

NADIR and RoCoF are depicted in Figure 9. In line with the results presented in Section 5.1.1, the **base control** provides the worst frequency response, with the minimum values of NADIR and RoCoF. The inertial contribution of both VSWTs and FESS improves those values. NADIR is specially improved with the **hybrid control**, whereas the **inertial control** improves the most the RoCoF values. Table 1 shows the load-shedding results. In more than 40% of the schedules (9/22) the load-shedding is activated with the **base control**, with one or two steps, and an averaged power shed of 0.93 MW. These schedules (numbers 1–8 and 11 in Table 2 of [53]) correspond with low wind power scenarios. VSPs and FSPs are not connected and thus, both FSPs mechanical inertia and VSPs synthetic inertia do not contribute to the grid frequency response. The **inertial control** improves 7 of the 9 schedules previously mentioned,

**TABLE 1** Load-shedding

Strategy	LS schedules	LS steps	$\overline{P_{shed}}$ (MW)
Base	9	1 & 2	0.93
Inertial	5	1 & 2	0.86
Hybrid	3	1	0.75
Hybrid & DB	3	1	0.75

decreasing the total amount of load to be shed (average power of 0.86 MW) and reducing the load-shedding activation up to 23% (5/22). With the two hybrid controls (**hybrid control** and **hybrid control with dead-band**), the same load-shedding results are obtained: the load shedding is improved in the 9 schedules and in only 13% of the schedules it was activated (schedules 3, 4, and 8 in Table 2 of [53] with both hybrid controls), with just one step, and an averaged power shed of 0.75 MW. These schedules correspond to high power demand scenarios. One of the schedules (number 2) in which load-shedding is totally avoided by using the hybrid controls is depicted in Figure 10. The load shedding reduction is a consequence of the substantial mitigation of the grid frequency deviations, with both hybrid controls. These low frequency excursions also address a minor hydro-power additional generation.

### 5.2 | Wear of elements

As was introduced in Section 1, it is commonly accepted that some elements' wear increase as vRES replaces conventional power plants. To verify this affirmation, we have analysed the relationship between the  $\overline{\Delta x}$  (which represents the wear of the hydro-power plants) and the number of cycles/h of FESS, with the wind integration in the 22 generation mix scenarios presented in Section 4. The **base control**, **hybrid control**, and **hybrid control with dead-band** are analysed for the  $\overline{\Delta x}$ , whereas for the number of cycles/h of FESS, the **base control** is not considered (as in that control FESS are not participating in the frequency regulation), but the **inertial control**. The results for the 22 generation mix scenarios are depicted in Figure 11. Note that there are 10 different initial

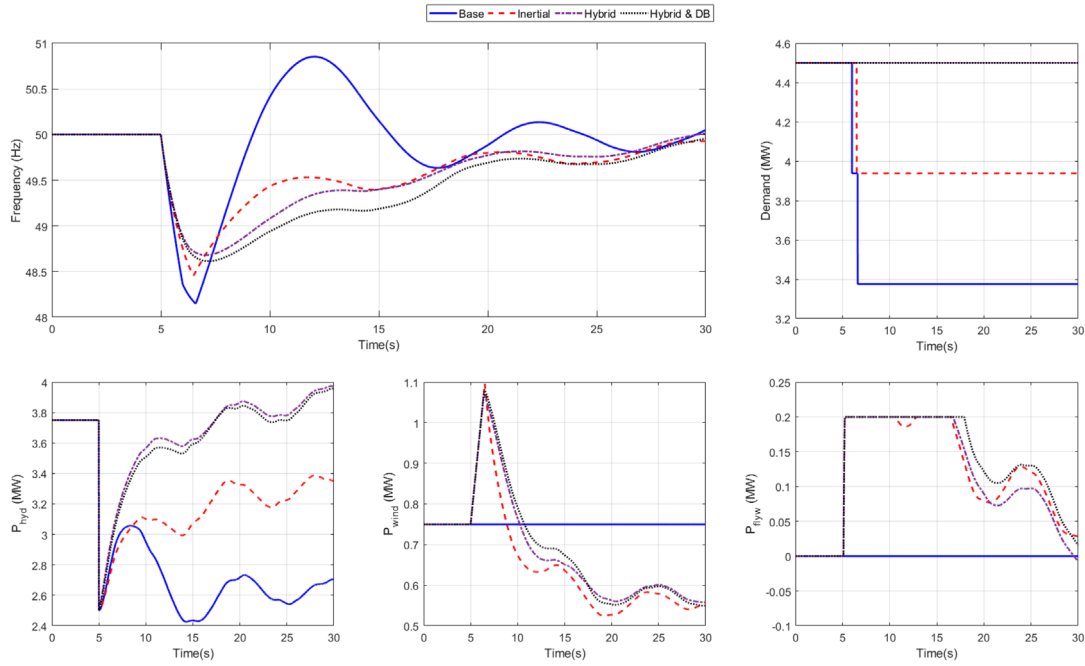


**FIGURE 10** Graphical results (grid frequency, power demand, and power supplied by the hydro units, VSWTs and FESS) with the outage of the 'largest generation unit'

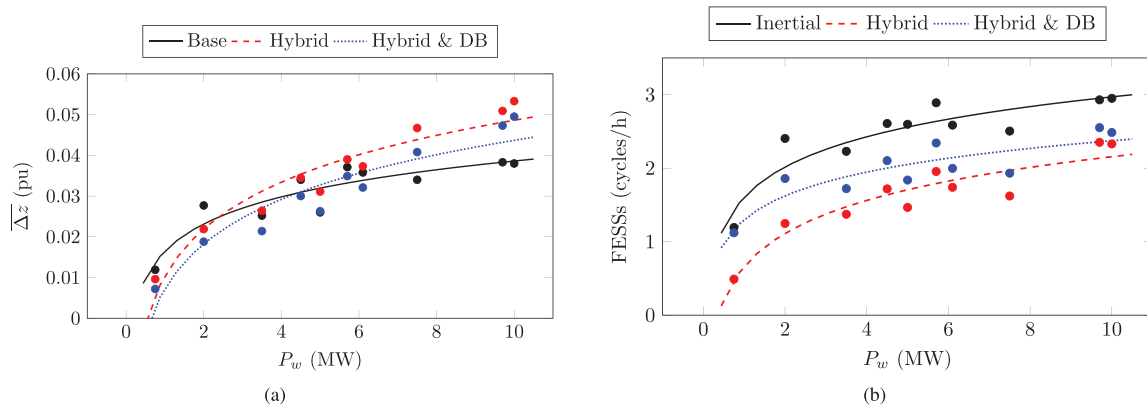


**FIGURE 11** Wear of elements. (a) Average nozzle deviation. (b) Number of cycles/h of FESSs.

wind power values from the 22 total generation mix scenarios. Consequently, such scenario results with the same initial wind power value have been aggregated into the average values. For the hydro-power plants (Figure 11a), an increase in the  $\overline{\Delta z}$  is gotten in all cases as the wind power increases. In fact, a logarithmic relationship represents such dependence between  $P_w$  and  $\overline{\Delta z}$ , with  $0.83 \leq R^2 \leq 0.93$ . Among the three control strategies, the **base control** gives the least wear, whereas the **hybrid control** has the highest. The **hybrid control with dead-band** gives an intermediate  $\overline{\Delta z}$ , as it could be expected. This fact is due to the dead-band slightly alleviates the hydro-power generation units participation in frequency control. For three of them, a severe increase is gotten between 0 and 2 MW of wind power, but then such increase is alleviated. With

regard to the number of cycles/h of FESS, it also increases as the wind power increases, refer to Figure 11b. Also a logarithmic relationship represents such dependence between  $P_w$  and number of cycles/h of FESSs, with  $0.77 \leq R^2 \leq 0.87$ . In this case, the **inertial control** is the most demanding strategy for the FESS, whereas the **hybrid control** is the least; as in the case of the  $\overline{\Delta z}$ , the **hybrid control with dead-band** lays in between. In this case, an important increase is gotten between 0 and 4 MW of wind power, but then the increase is slower. Authors would like to emphasise that the relationship between the wear (both for hydro-power plants and FESS) with the wind power integration is logarithmic, not linear. Consequently, the different elements' wear will substantially increase for low wind integration (or, in general, vRES integration), but this increase

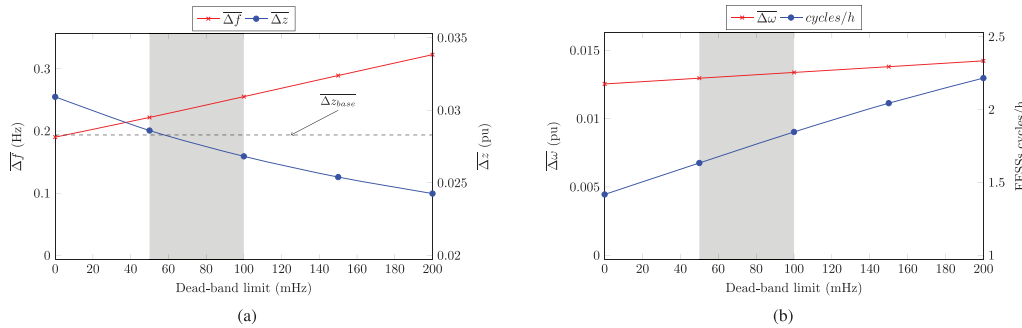


**FIGURE 12** Dead-band values: relationships. (a) Average frequency deviation, hydro's wear and dead-band. (b) Average rotational speed deviation, cycles per hour and dead-band.

stabilises as the integration of vRES is higher. This means that doubling the integration of vRES does not imply to double the wear, as it is not a linear relationship.

### 5.3 | Analysis of the dead-band value

As can be seen in Figure 4, and presented in Section 3.3, a dead-band is included in the hybrid hydro-wind-flywheel frequency control strategy. Five different values of the dead-band are considered in this study (0,  $\pm 50$ ,  $\pm 100$ ,  $\pm 150$ , and  $\pm 200$  mHz), to determine the average frequency deviation ( $\overline{\Delta f}$ ), nozzle deviations ( $\overline{\Delta z}$ ), rotational speed deviation of VSWTs ( $\overline{\Delta \omega}$ ), and the cycles per hour of the FESS (FESS cycles/h). In this way, it is possible to see how the dead-band affects the different parameters under analysis. They are depicted in Figure 12. It can be seen that the minimum values of  $\overline{\Delta f}$ ,  $\overline{\Delta \omega}$  and the FESS' number of cycles/h correspond to a dead-band of 0 mHz (i.e. there is no dead-band), which is the **hybrid control** between hydro-wind-flywheels. However, this hybrid strategy causes the  $\overline{\Delta z}$  of the hydro-power plant to be the maximum value. Consequently, to try to mitigate the hydro-power plants' wear, a different value from 0 should be used in the dead-band. By increasing the dead-band limit from 0 to 200 mHz:

- $\overline{\Delta f}$  increases nearly a 70% (from 0.1902 Hz to 0.3228 Hz)
- $\overline{\Delta z}$  reduces more than 20% (from 0.0309 pu to 0.0243 pu)
- $\overline{\Delta \omega}$  increases around 14% (from 0.0125 pu to 0.0142 pu)
- Number of cycles/h of FESS increases nearly a 60% (1.4174 cycles/h to 2.2160 cycles/h)

Consequently, by increasing the value of the dead-band, the hydro-power plants' wear is reduced, but the average frequency deviations, rotational speed of VSWTs, and number of cycles per hour increase accordingly. With this, it is possible to get an idea of how much it can be saved on some parameters by getting worse the rest of them. To determine which value to use in the present study, authors have considered the  $\overline{\Delta z}$  of the **base control** (when neither VSWTs nor FESS participate in grid frequency control). Such value is  $\overline{\Delta z} = 0.0283$ , as shown

in black dashed line in Figure 12. Therefore, comparing the  $\overline{\Delta z}$  values of Figure 12 to the  $\overline{\Delta z}_{base}$  of the **base control**, the optimum value of the dead-band limit is in between  $\pm 50$  and  $\pm 100$  mHz, as shaded in Figure 12. Within this range, a similar  $\overline{\Delta z} \approx \overline{\Delta z}_{base}$  is obtained for hydro-power generating units ( $+1\%$  at 50 mHz and  $-5\%$  at 100 mHz), comparing to the  $\overline{\Delta z}_{base}$  value. At the same time,  $\overline{\Delta f}$ ,  $\overline{\Delta \omega}$ , and the number of cycles per hour of FESSs does not increase excessively in comparison to not including a dead-band ( $+34\%$ ,  $+7\%$ , and  $+30\%$  for the 100 mHz dead-band value, respectively). Note that these increases are related to the **hybrid control**, not the **base control**. According to these results, if a lower value for the dead-band had been chosen in Section 5.1, all the parameters related to frequency ( $\overline{\Delta f}$ , NADIR, and RoCoF), together with  $\overline{\Delta \omega}$  and the number of cycles per hour of FESS, would have gotten better results (closer to the **hybrid control**), whereas  $\overline{\Delta z}$  would have been worse. By this means, and selecting the 100 mHz dead-band, the results provided in Section 5.1 are the best in terms of  $\overline{\Delta z}$ , and the 'worst' in terms of  $\overline{\Delta f}$ ,  $\overline{\Delta \omega}$ , and FESS cycles per hour. A multi-criteria analysis including economic aspects related to the wear of the elements and the grid frequency regulation should be developed as a future work to properly determine the optimum value of the dead-band in each case.

## 6 | CONCLUSION

Grid control and operation should include an active role for wind energy due to its relevant integration into current power systems. With this aim, this paper proposes a hybrid hydro-wind-flywheel frequency control strategy for isolated power systems with 100% renewable energy generation mix scenarios, conducted to reduce hydro-power plant's, VSWTs and FESS wear, maintaining minor grid frequency excursions. VSWTs and flywheels include a conventional inertial frequency control. In addition to the frequency deviation, the hydro-power controller also tracks the VSWTs' rotational speed deviation and the SOC of the flywheels to modify the generated power accordingly. In this way, a grid frequency excursion dead-band is included

to avoid excessive hydro-power plant participation in grid frequency regulation. Hybrid frequency controls provide considerably lower frequency excursions under wind speed oscillations and loss of the largest generation plant in comparison to previous frequency controllers. In fact, the averaged frequency deviations are reduced by around 50% with the proposed hybrid controller when wind speed fluctuations are simulated. Load-shedding are also significantly reduced (from 40% to 13% of the generation mix scenarios) with the proposed hybrid controller when the loss of the largest power generator is considered for simulation. A dead-band analysis has been carried out to optimise this value according to frequency excursions, hydro-power generation units' wear, wind turbine rotational speed deviations, and flywheel cycles per hour. A trade-off among these four parameters is achieved with dead-band values between  $\pm 50$  and  $\pm 100$  mHz. From the results, this dead-band reduces the wear of hydro power plant components at a cost of increasing the number of flywheel cycles per hour. The increment of cycles does not compromise the FESS remaining lifetime. A detailed multi-criteria analysis should be developed as a future work, including economic aspects related to the wear of the elements and the grid frequency regulation. Additionally, a combined hybrid frequency control considering other renewables, such as PV power plants, is currently a field of interest by the authors for potential future works.

## ACKNOWLEDGEMENTS

The work presented in this paper was partially funded by the 'Consejería de Ciencia, Universidad e Innovación' of Comunidad de Madrid (Spain) under the project 'Sizing and control of flywheel energy storage power plants in isolated power systems with high renewable penetration' of the 'Convenio plurianual entre la Comunidad de Madrid y la Universidad Politécnica de Madrid (Ref. APOYO-JOVENES-SU3JLM-61-6XFZ49)'. The work was also partially supported by the Council of Communities of Castilla-La Mancha, Spain (Ref. SBPLY/19/180501/000287) and the European Union FEDER. In addition, PhD Ana Fernández-Guillamón would like to thank Spanish SEPE (Spanish National Unemployment System) for its funding support.

## CONFLICT OF INTEREST

The authors declare no conflict of interest.

## NOMENCLATURE

AGC	Automatic generation control
ESS	Energy storage system
FESS	Flywheel energy storage system
FSP	Fixed speed pump
MPPT	Maximum power point tracking
NADIR	Minimum frequency value
PD	Proportional derivative
PI	Proportional integral
PID	Proportional integral derivative
RES	Renewable energy sources
RoCoF	Rate of change of frequency
SOC	State of charge

UFLS	Under frequency load shedding
UNESCO	United Nations Educational, Scientific, and Cultural Organisation
VSP	Variable speed pump
vRES	Variable renewable energy sources
VSWT	Variable speed wind turbine
$\omega$	Rotational speed of VSWTs
$\omega_{ref}$	Reference rotational speed of VSWTs
$\frac{\Delta f}{f}$	Average frequency deviation
$\Delta p_{FESS}$	Variation of active power of FESS
$\Delta p_w$	Variation of active power of VSWTs
$\Delta p_{w,f}$	Variation of active power of VSWTs provided by VSWTs inertial control loop
$\Delta p_{w,\omega}$	Power reference provided by VSWTs speed control loop
$\frac{\Delta \omega}{\omega}$	Average rotational speed deviation of VSWTs
$\frac{\Delta x}{x}$	Average hydro-power generation units' wear
$\Delta SOC$	Average state of charge deviation of FESS
$f$	Frequency [Hz]
$f_{ref}$	Reference frequency [1 p.u.]
$p_b$	Power generated by hydroelectric units [p.u.]
$p_w$	Power generated by VSWTs [p.u.]
$p_D$	Power consumed by consumers [p.u.]
$p_{FSP}$	Power consumed by FSPs [p.u.]
$p_{VSP}$	Power consumed by VSPs [p.u.]
$s_w$	Wind speed [m/s]
$D_{net}$	Load sensitive parameter to frequency deviations
$H_b$	Inertia constant of hydro-electric units [s]
$K_{d,F}$	Derivative constant of FESS
$K_{d,VSP}$	Derivative constant of VSPs
$K_{d,wf}$	Derivative constant of VSWTs
$K_{i,w\omega}$	Integral constant of VSWTs speed control loop
$K_{i,VSP}$	Integral constant of VSPs
$K_{p,w\omega,byd}$	Proportional constant of the hybrid control between $\omega$ and hydro-electric units
$K_{p,VSP}$	Proportional constant of VSPs
$K_{p,wf}$	Proportional constant of VSWTs
$K_{p,\omega}$	Proportional constant of VSWTs speed control loop
$K_{p,F}$	Proportional constant of FESS
$K_{p,soc,byd}$	Proportional constant of the hybrid control between SOC and hydro-electric units
$P_{flyw}$	Flywheels active power [MW]
$P_{byd}$	Hydro-electric active power [MW]
$P_{wind}$	VSWTs active power [MW]

## ORCID

Guillermo Martínez-Lucas  <https://orcid.org/0000-0002-3993-6223>

Ángel Molina-García  <https://orcid.org/0000-0001-6824-8684>

## REFERENCES

1. Fernández Guillamón, A., Das, K., Cutululis, N.A., Molina García, Á.: Off-shore wind power integration into future power systems: Overview and trends. *J. Mar. Sci. Eng.* 7(11), 399 (2019)
2. Gil García, I.C., García Cascales, M.S., Fernández Guillamón, A., Molina García, A.: Categorization and analysis of relevant factors for optimal



- locations in onshore and offshore wind power plants: A taxonomic review. *J. Mar. Sci. Eng.* 7(11), 391 (2019)
3. Molina García, A., Fernández Guillamón, A., Gómez Lázaro, E., Honrubia Escribano, A., Bueso, M.C.: Vertical wind profile characterization and identification of patterns based on a shape clustering algorithm. *IEEE Access* 7, 30890–30904 (2019)
  4. Fernández Guillamón, A., Sarasúa, J.I., Chazarra, M., Viguera Rodríguez, A., Fernández Muñoz, D., Molina García, Á.: Frequency control analysis based on unit commitment schemes with high wind power integration: A spanish isolated power system case study. *Int. J. Electr. Power Energy Syst.* 121, 106044 (2020)
  5. Tielens, P., Van Hertem, D.: The relevance of inertia in power systems. *Renew. Sustain. Energy Rev.* 55, 999–1009 (2016)
  6. Fernández Guillamón, A., Gómez Lázaro, E., Molina García, Á.: Extensive frequency response and inertia analysis under high renewable energy source integration scenarios: application to the european interconnected power system. *IET Renew. Power Gener.* 14(15), 2885–2896 (2020)
  7. Fernández Guillamón, A., Gómez Lázaro, E., Muljadi, E., Molina García, Á.: Power systems with high renewable energy sources: A review of inertia and frequency control strategies over time. *Renew. Sustain. Energy Rev.* 115, 109369 (2019)
  8. Fernández Guillamón, A.: New contributions to frequency control based on virtual synchronous generators: Application to power systems with high renewable energy sources integration. *Universidad Politécnica de Cartagena* (2020)
  9. Hewicker, C., Hogan, M., Mogren, A.: *Power Perspectives 2030: On the Road to a Decarbonised Power Sector*. The European Climate Foundation, Hague (2011)
  10. Australian Energy Market Operator Limited: 2020 integrated system plan, (AEMO). <https://www.aemo.com.au/-/media/files/major-publications/isp/2020/final-2020-integrated-system-plan.pdf>. Last accessed date: 1 October 2021
  11. Kuwahata, R., Merk, P., Wakeyama, T., Pescia, D., Rabe, S., Ichimura, S.: Renewables integration grid study for the 2030 japanese power system. *IET Renew. Power Gener.* 14(8), 1249–1258 (2020)
  12. Luo, Y., Shi, L., Tu, G.: Optimal sizing and control strategy of isolated grid with wind power and energy storage system. *Energy Convers. Manage.* 80, 407–415 (2014)
  13. Edmunds, R., Davies, L., Deane, P., Pourkashanian, M.: Thermal power plant operating regimes in future british power systems with increasing variable renewable penetration. *Energy Convers. Manage.* 105, 977–985 (2015)
  14. Yang, W., Norrnlund, P., Saarinen, L., Yang, J., Guo, W., Zeng, W.: Wear and tear on hydro power turbines—influence from primary frequency control. *Renewable Energy* 87, 88–95 (2016)
  15. Yang, W., Norrnlund, P., Saarinen, L., Yang, J., Zeng, W., Lundin, U.: Wear reduction for hydropower turbines considering frequency quality of power systems: a study on controller filters. *IEEE Trans. Power Syst.* 32(2), 1191–1201 (2016)
  16. Saarinen, L., Norrnlund, P., Yang, W., Lundin, U.: Linear synthetic inertia for improved frequency quality and reduced hydropower wear and tear. *Int. J. Electr. Power Energy Syst.* 98, 488–495 (2018)
  17. Yang, W., Norrnlund, P., Saarinen, L., Witt, A., Smith, B., Yang, J., et al.: Burden on hydropower units for short-term balancing of renewable power systems. *Nat. Commun.* 9(1), 1–12 (2018)
  18. Fini, M.H., Golshan, M.E.H.: Frequency control using loads and generators capacity in power systems with a high penetration of renewables. *Electr. Power Syst. Res.* 166, 43–51 (2019)
  19. Dekka, A., Ghaffari, R., Venkatesh, B., Wu, B.: A survey on energy storage technologies in power systems. In: 2015 IEEE Electrical Power and Energy Conference (EPEC), pp. 105–111. (2015)
  20. Wang, D., Gao, X., Meng, K., Qiu, J., Lai, L.L., Gao, S.: Utilisation of kinetic energy from wind turbine for grid connections: a review paper. *IET Renew. Power Gener.* 12, 615–624(9) (2018)
  21. Soliman, M.A., Hasanien, H.M., Azazi, H.Z., El-kholy, E.E., Mahmoud, S.A.: Hybrid anfis-ga-based control scheme for performance enhancement of a grid-connected wind generator. *IET Renew. Power Gener.* 12, 832–843(11) (2018)
  22. Fernández Guillamón, A., Viguera Rodríguez, A., Molina García, Á.: Analysis of power system inertia estimation in high wind power plant integration scenarios. *IET Renew. Power Gener.* 13(15), 2807–2816 (2019)
  23. Vasudevan, K.R., Ramchandaramurthy, V.K., Venugopal, G., Ekanayake, J.B., Tiong, S.K.: Variable speed pumped hydro storage: A review of converters, controls and energy management strategies. *Renew. Sustainable Energy Rev.* 135, 110156 (2021)
  24. Li, X., Anvari, B., Palazzolo, A., Wang, Z., Toliyat, H.: A utility-scale flywheel energy storage system with a shaftless, hubless, high-strength steel rotor. *IEEE Trans. Ind. Electron.* 65(8), 6667–6675 (2018)
  25. Delille, G., Francois, B., Malarange, G.: Dynamic frequency control support by energy storage to reduce the impact of wind and solar generation on isolated power system's inertia. *IEEE Trans. Sustain. Energy* 3(4), 931–939 (2012)
  26. Mousavi G, S.M., Faraji, F., Majazi, A., Al Haddad, K.: A comprehensive review of flywheel energy storage system technology. *Renew. Sustain. Energy Rev.* 67, 477–490 (2017)
  27. Olabi, A.G., Wilberforce, T., Abdelkareem, M.A., Ramadan, M.: Critical review of flywheel energy storage system. *Energies* 14(8), 2159 (2021)
  28. Amiryar, M.E., Pullen, K.R.: A review of flywheel energy storage system technologies and their applications. *Appl. Sci.* 7(3), 286 (2017)
  29. Kesgin, M.G., Han, P., Taran, N., Ionel, D.M.: Overview of flywheel systems for renewable energy storage with a design study for high-speed axial-flux permanent-magnet machines. In: 2019 8th International Conference on Renewable Energy Research and Applications (ICRERA), pp. 1026–1031. IEEE, Piscataway (2019)
  30. Goris, F., Severson, E.L.: A review of flywheel energy storage systems for grid application. In: IECON 2018-44th Annual Conference of the IEEE Industrial Electronics Society, pp. 1633–1639. IEEE, Piscataway (2018)
  31. Mir, A.S., Senroy, N.: Intelligently controlled flywheel storage for enhanced dynamic performance. *IEEE Trans. Sustain. Energy* 10(4), 2163–2173 (2019)
  32. Taj, T.A., Hasanien, H.M., Alolah, A.I., Mueeen, S.M.: Transient stability enhancement of a grid-connected wind farm using an adaptive neuro-fuzzy controlled-flywheel energy storage system. *IET Renew. Power Gener.* 9, 792–800(8) (2015)
  33. Yao, J., Yu, M., Gao, W., Zeng, X.: Frequency regulation control strategy for pmsg wind-power generation system with flywheel energy storage unit. *IET Renew. Power Gener.* 11(8), 1082–1093 (2017)
  34. Zhang, F., Tokombayev, M., Song, Y., Gross, G.: Effective flywheel energy storage (fes) offer strategies for frequency regulation service provision. In: 2014 Power Systems Computation Conference, pp. 1–7. IEEE, Piscataway (2014)
  35. Peralta, D., Cañizares, C., Bhattacharya, K.: Practical modeling of flywheel energy storage for primary frequency control in power grids. In: 2018 IEEE Power Energy Society General Meeting (PESGM), pp. 1–5. IEEE, Piscataway (2018)
  36. Pérez Diaz, J.L., Lafoz, M., Burke, F.: Integration of fast acting energy storage systems in existing pumped-storage power plants to enhance the system's frequency control. *Wiley Interdiscip. Rev.: Energy Environ.* 9(2), e367 (2020)
  37. Silva Saravia, H., Pulgar Painemal, H., Mauricio, J.M.: Flywheel energy storage model, control and location for improving stability: The chilean case. *IEEE Trans. Power Syst.* 32(4), 3111–3119 (2017)
  38. Dar, S.Z.N., Baraniya, S.: Integration of flywheel energy storage to AGC of two area power system. In: 2020 IEEE Bangalore Humanitarian Technology Conference (B-HTC), pp. 1–4. IEEE, Piscataway (2020)
  39. Abazari, A., Monsef, H., Wu, B.: Coordination strategies of distributed energy resources including FESS, DEG, FC and WTG in load frequency control (LFC) scheme of hybrid isolated micro-grid. *Int. J. Electr. Power Energy Syst.* 109, 535–547 (2019)
  40. Gayathri, N.S., Senroy, N., Kar, I.N.: Smoothing of wind power using flywheel energy storage system. *IET Renew. Power Gener.* 11(3), 289–298 (2017)
  41. Wu, Z., Gao, W., Gao, T., Yan, W., Zhang, H., Yan, S., et al.: State-of-the-art review on frequency response of wind power plants in power systems. *J. Modern Power Syst. Clean Energy* 6(1), 1–16 (2018)

42. Akram, U., Nadarajah, M., Shah, R., Milano, F.: A review on rapid responsive energy storage technologies for frequency regulation in modern power systems. *Renew. Sustain. Energy Rev.* 120, 109626 (2020)
43. Hungerford, Z., Bruce, A., MacGill, I.: The value of flexible load in power systems with high renewable energy penetration. *Energy* 188, 115960 (2019)
44. Karbouj, H., Rather, Z.H., Flynn, D., Qazi, H.W.: Non-synchronous fast frequency reserves in renewable energy integrated power systems: A critical review. *Int. J. Electr. Power Energy Syst.* 106, 488–501 (2019)
45. Mansoor, S., Jones, D., Bradley, D.A., Aris, F., Jones, G.: Reproducing oscillatory behaviour of a hydroelectric power station by computer simulation. *Control Eng. Pract.* 8(11), 1261–1272 (2000)
46. Sarasúa, J.I., Martínez Lucas, G., Lafoz, M.: Analysis of alternative frequency control schemes for increasing renewable energy penetration in el hierro island power system. *Int. J. Electr. Power Energy Syst.* 113, 807–823 (2019)
47. O'Sullivan, J., Rogers, A., Flynn, D., Smith, P., Mullane, A., O'Malley, M.: Studying the maximum instantaneous non-synchronous generation in an island system—frequency stability challenges in ireland. *IEEE Trans. Power Syst.* 29(6), 2943–2951 (2014)
48. Martínez Lucas, G., Sarasúa, J.I., Sánchez Fernández, J.Á., Wilhelmi, J.R.: Power-frequency control of hydropower plants with long penstocks in isolated systems with wind generation. *Renew. Energy* 83, 245–255 (2015)
49. Fernández Muñoz, D., Pérez Díaz, J.I., Chazarra, M.: A two-stage stochastic optimisation model for the water value calculation in a hybrid diesel/wind/pumped-storage power system. *IET Renew. Power Gener.* 13(12), 2156–2165 (2019)
50. Martínez Lucas, G., Sarasúa, J.I., Sánchez Fernández, J.Á.: Frequency regulation of a hybrid wind–hydro power plant in an isolated power system. *Energies* 11(1), 239 (2018)
51. Liu, J., Wen, J., Yao, W., Long, Y.: Solution to short-term frequency response of wind farms by using energy storage systems. *IET Renew. Power Gener.* 10, 669–678(9) (2016)
52. Sarasúa, J.I., Martínez Lucas, G., Platero, C.A., Sánchez Fernández, J.Á.: Dual frequency regulation in pumping mode in a wind–hydro isolated system. *Energies* 11(11), 2865 (2018)
53. Martínez Lucas, G., Sarasúa, J.I., Pérez Díaz, J.I., Martínez, S., Ochoa, D.: Analysis of the implementation of the primary and/or inertial frequency control in variable speed wind turbines in an isolated power system with high renewable penetration. case study: El hierro power system. *Electronics* 9(6), 901 (2020)
54. Miller, N.W., Sanchez Gasca, J.J., Price, W.W., Delmerico, R.W.: Dynamic modeling of ge 1.5 and 3.6 mw wind turbine-generators for stability simulations. In: 2003 IEEE Power Engineering Society General Meeting (IEEE Cat. No. 03CH37491), vol. 3, pp. 1977–1983. IEEE, Piscataway (2003)
55. Clark, K., Miller, N.W., Sanchez Gasca, J.J.: Modeling of ge wind turbine-generators for grid studies. *GE Energy* 4, 0885–8950 (2010)
56. Zhao, S., Nair, N.K.: Assessment of wind farm models from a transmission system operator perspective using field measurements. *IET Renew. Power Gener.* 5(6), 455–464 (2011)
57. Sarasúa, J.I., Martínez Lucas, G., Pérez Díaz, J.I., Fernández Muñoz, D.: Alternative operating modes to reduce the load shedding in the power system of El Hierro island. *Int. J. Electr. Power Energy Syst.* 128, 106755 (2021)
58. Sarasúa, I., Torres, B., Pérez Díaz, J., Lafoz, M.: Control strategy and sizing of a flywheel energy storage plant for the frequency control of an isolated power system. In: 15th Wind Integration Workshop. Energynautics GmbH, Darmstadt (2016)
59. Torres, J., Moreno Torres, P., Navarro, G., Blanco, M., Lafoz, M.: Fast energy storage systems comparison in terms of energy efficiency for a specific application. *IEEE Access* 6, 40656–40672 (2018)
60. Mauricio, J.M., Marano, A., Gómez Expósito, A., Ramos, J.L.M.: Frequency regulation contribution through variable-speed wind energy conversion systems. *IEEE Trans. Power Syst.* 24(1), 173–180 (2009)
61. Menezes, E.J.N., Araújo, A.M., da Silva, N.S.B.: A review on wind turbine control and its associated methods. *J. Cleaner Prod.* 174, 945–953 (2018)
62. Hilal, M., Maaroufi, M., Ouassaid, M.: Doubly fed induction generator wind turbine control for a maximum power extraction. In: 2011 International Conference on Multimedia Computing and Systems. pp. 1–7. IEEE, Piscataway (2011)
63. Hansen, A.D., Altin, M., Margaris, I.D., Iov, F., Tarnowski, G.C.: Analysis of the short-term overproduction capability of variable speed wind turbines. *Renew. Energy* 68, 326–336 (2014)
64. Fernández Guillamón, A., Martínez Lucas, G., Molina García, Á., Sarasua, J.I.: An adaptive control scheme for variable speed wind turbines providing frequency regulation in isolated power systems with thermal generation. *Energies* 13(13), 3369 (2020)
65. Takahashi, R., Tamura, J.: Frequency control of isolated power system with wind farm by using flywheel energy storage system. In: 2008 18th International Conference on Electrical Machines, pp. 1–6. IEEE, Piscataway (2008)
66. Fernández Guillamón, A., Martínez Lucas, G., Molina García, Á., Sarasua, J.I.: Hybrid wind–pv frequency control strategy under variable weather conditions in isolated power systems. *Sustainability* 12(18), 7750 (2020)
67. Martínez Lucas, G., Sarasua, J.I., Fernández Guillamón, A., Molina García, Á.: Combined hydro–wind frequency control scheme: Modal analysis and isolated power system case example. *Renew. Energy* 180, 1056–1072 (2021)
68. Martínez Lucas, G., Sarasúa, J.I., Sánchez Fernández, J.Á.: Eigen analysis of wind–hydro joint frequency regulation in an isolated power system. *I. J. Electr. Power Energy Syst.* 103, 511–524 (2018)
69. Quevedo, A.M., Domínguez, E.J.M., de León Izquier, J.M., de León, R.C., Arozarena, P.S., Moreno, J.G., et al.: Gorona del viento wind-hydro power plant. In: 3rd International Hybrid Power Systems Workshop. Energynautics GmbH, Darmstadt (2018)
70. Perez Diaz, J.I., Sarasua, J.I., Wilhelmi, J.R.: Contribution of a hydraulic short-circuit pumped-storage power plant to the load–frequency regulation of an isolated power system. *Int. J. Electr. Power Energy Syst.* 62, 199–211 (2014)
71. Nichita, C., Luca, D., Dakyo, B., Ceanga, E.: Large band simulation of the wind speed for real time wind turbine simulators. *IEEE Trans. Energy Convers.* 17(4), 523–529 (2002)
72. Van der Hoven, I.: Power spectrum of horizontal wind speed in the frequency range from 0.0007 to 900 cycles per hour. *J. Atmos. Sci.* 14(2), 160–164 (1957)
73. Leithead, W., De la Salle, S., Reardon, D.: Role and objectives of control for wind turbines. In: IEE Proceedings C-Generation, Transmission and Distribution, vol. 138, pp. 135–148. IET, (1991)
74. Persson, M., Chen, P.: Frequency control by variable speed wind turbines in islanded power systems with various generation mix. *IET Renewable Power Gener.* 11(8), 1101–1109 (2017)
75. Díaz González, F., Sumpster, A., Gomis Bellmunt, O., Villafáfila Robles, R.: A review of energy storage technologies for wind power applications. *Renew. Sustain. Energy Rev.* 16(4), 2154–2171 (2012)
76. Marzband, M., Moghaddam, M.M., Akorede, M.F., Khomeyrani, G.: Adaptive load shedding scheme for frequency stability enhancement in micro-grids. *Electr. Power Syst. Res.* 140, 78–86 (2016)

**How to cite this article:** Sarasua, J.I., Martínez-Lucas, G., García-Pereira, H., Navarro-Soriano, G., Molina-García, Á., Fernández-Guillamón, A.: Hybrid frequency control strategies based on hydro-power, wind, and energy storage systems: Application to 100% renewable scenarios. *IET Renew. Power Gener.* 16, 1107–1120 (2022). <https://doi.org/10.1049/rpg2.12326>